Progress In Electromagnetics Research B, Vol. 45, 101–116, 2012

A MICROSTRIP ANTENNA WITH A RECONFIGURABLE PATTERN FOR RFID APPLICATIONS

G. Monti*, L. Corchia, and L. Tarricone

Department of Engineering for Innovation, University of Salento, Via per Monteroni, Lecce 73100, Italy

Abstract—This paper presents a low-cost patternreconfigurable microstrip antenna. The proposed design strategy uses a slotted patch antenna on a bi-layer structure as basic element of a switched parasitic array. Reconfigurability is obtained by means of PIN diodes used to vary the resonance frequency of the parasitic patches. Experimental results referring to a prototype consisting of an array of three elements optimized for the Ultra High Frequency (UHF) band of Radio Frequency IDentification (RFID) systems are presented and discussed. It is demonstrated that the proposed antenna exhibits a main beam that can be reconfigured into three different directions.

1. INTRODUCTION

Reconfigurable antennas and devices [1–9] represent a key technology for improving the performance of wireless communication systems. Accordingly, several design strategies for achieving reconfigurabilty in terms of one or more antenna parameters (i.e., operating frequency, polarization, etc.) have been proposed in the literature [7–16]. Among these, antennas with a reconfigurable radiation pattern are of great interest due to their positive impact on network capacity and reliability by reducing interference problems and maximizing signal-to-noise ratio. To this regard, particularly attractive are Switched Parasitic Arrays (SPAs). In fact, differently from adaptive arrays [17–19], SPAs do not require multiple and/or reconfigurable RF channels: the pattern reconfigurability is obtained by loading the active antenna with reconfigurable parasitic elements [20]. As a consequence, SPAs are suitable to be implemented at a lower cost and smaller size, thus representing an excellent candidate to be used in mobile terminals/nodes and low-cost applications.

Received 8 September 2012, Accepted 18 October 2012, Scheduled 24 October 2012

* Corresponding author: Giuseppina Monti (giuseppina.monti@unisalento.it).

The first SPAs proposed in the literature, were three-dimensional structures using monopoles [21–23]. More recently, some low-profile devices have been proposed [24–26].

In this paper the use of a slotted microstrip patch antenna as basic element of an SPA is investigated. The pattern reconfigurability is implemented by means of PIN diodes used to vary the length of the slot on the diagonal of the parasitic patches. A prototype consisting of an array of three elements optimized for the UHF band of RFID systems [27–33] has been realized and characterized. From experimental data, it is demonstrated that the device here presented is able to reconfigure the main beam direction in the H-plane. The main advantages related to the proposed approach are: a low profile, low-cost, high values of the directivity, the possibility of using design strategies commonly adopted for microstrip patch antennas to obtain compact dimensions and to govern the antenna polarization [10, 32, 34–36].

2. SWITCHED PARASITIC ARRAY: DESIGN STRATEGY

The general architecture of an SPA is illustrated in Fig. 1. The basic idea is to load the active antenna with parasitic elements. Reconfigurability is obtained by using PIN diodes or variable reactive loads (such as varactors) to reconfigure the resonance frequency of the parasitic antennas.

The idea here suggested consists in using a compact patch antenna as basic element of the array (see Fig. 2). More details about the design process of the active and parasitic patches are given in the following part of this section.

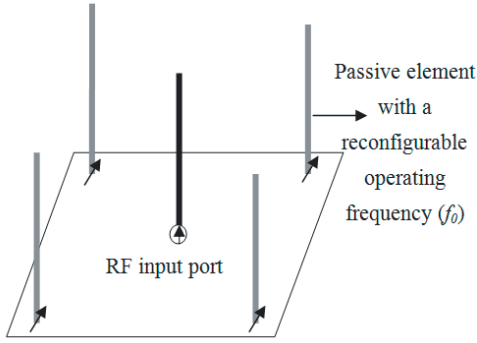

Figure 1. General architecture of the switched parasitic array proposed in [23].

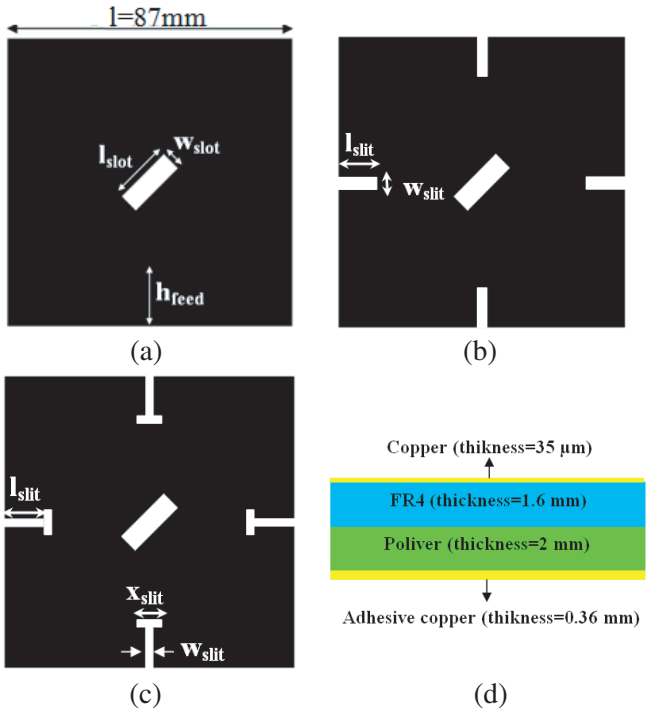

Figure 2. Comparison between different patch geometries obtained by applying rectangular slots to a conventional square patch. (a) Square patch with a rectangular slot on the diagonal; (b) square patch with a rectangular slot on the diagonal and four rectangular slits orthogonal to the patch boundary. (c) and (d) Patch used as active element of the proposed SPA: (c) front view, (d) side view.

2.1. Active Patch Design

The patch used as active element of the proposed SPA is illustrated in Fig. 2(c). It is positioned on a bi-layer consisting of a single-sided copper clad FR4 laminate ($\varepsilon_r = 3.7$, $\tan(\delta) = 0.019$, thickness = 1.6 mm) and a poliver layer ($\varepsilon_r = 2.5$, $\tan(\delta) = 0.01$, thickness = 2 mm); the ground plane was realized by means of adhesive copper (thickness = 0.36 mm). As for the patch geometry, in order to obtain an elliptical polarization and compact dimensions, a rectangular slot and four t-shaped slits were applied to the patch diagonal and to the patch boundary [37], respectively. Fig. 3 compares the reflection coefficients of a simple square patch with the ones corresponding to the same patch with: a slot on the diagonal (see Fig. 2(a)), a slot on the diagonal and rectangular slits on the edges (see Fig. 2(b)), a slot on the diagonal and t-shaped slits on the edges (see Fig. 2(c)).

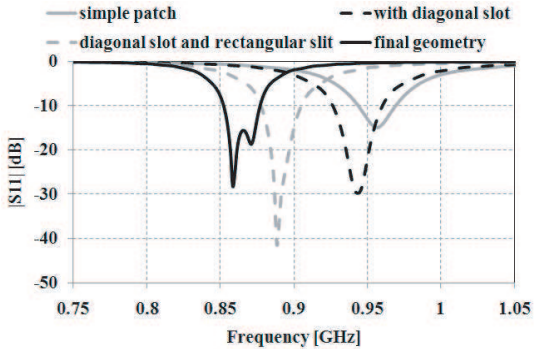

Figure 3. Comparison among the reflection coefficient calculated for the patches illustrated in Fig. 2.

Table 1. Dimensions of the patches used in the realized SPA.

Active patch dimensions [mm]									
		l	$\mathbf{l_{slot}}$	$\mathbf{w_{slot}}$	$\mathbf{h_{feed}}$	$\mathbf{l_{slit}}$	$\mathbf{w_{slit}}$	$\mathbf{x_{slit}}$	
		87	18.7	6.5	26	13.8	1.6	7.4	
Passive patch dimensions [mm]									
l	$\mathbf{l_r}$	$\mathbf{w_r}$	$\mathbf{l_d}$	$\mathbf{w_d}$	$\mathbf{l_{slit}}$	$\mathbf{w_{slit}}$	$\mathbf{x_{slit}}$	$\mathbf{gap_1}$	$\mathbf{gap_2}$
87	28.6	8.4	11.8	6.1	13.8	1.6	7.4	0.9	0.75

It can be seen that, with respect to a conventional patch, the combined use of a slot on the diagonal and t-shaped slits allows to obtain a size reduction. In fact from Fig. 3 it can be noticed that, with respect to a conventional square patch, the geometry illustrated in Fig. 2(c) exhibits a lower frequency of resonance. More specifically, the size reduction is of about 11%. All parameters of the patch geometry illustrated in Fig. 2(c) were optimized for operation at 866 MHz. The full-wave simulator CST Microwave Studio and proprietary tools [38–42] were used for optimizations; the dimensions of the final geometry calculated this way are given in Table 1.

Figure 4(a) shows a photograph of the realized prototype; the measured reflection coefficient is given in Fig. 4(b) and compared with numerical data. The patch exhibits a bandwidth of about 20 MHz ($|S_{11}| < -10$ dB in the frequency range 853.6–873 MHz). As for the radiation properties, numerical results are illustrated in Fig. 5; the patch has a broadside radiation pattern with a maximum of the gain of about 5 dBi. According to Fig. 4(b), where it can be seen that the operating frequency of 866 MHz is between the resonance frequencies of the two orthogonal modes due to the presence of the diagonal slot,

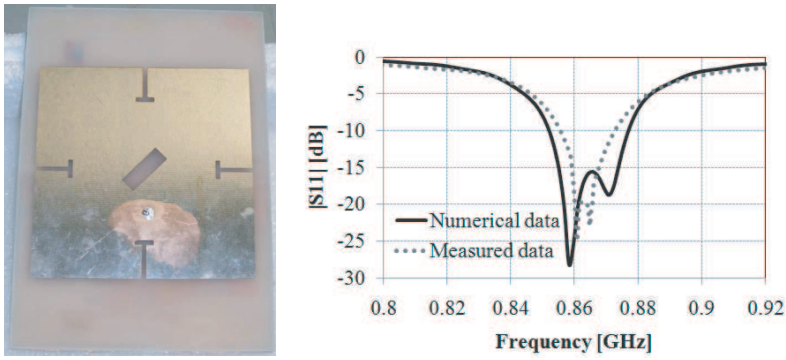

(a) (b)

Figure 4. Results obtained for the geometry illustrated in Fig. 2(c); the dimensions were optimized for operation at 866 MHz. (a) Photograph of the realized prototype, (b) comparison between full-wave simulations and experimental data obtained for the reflection coefficient.

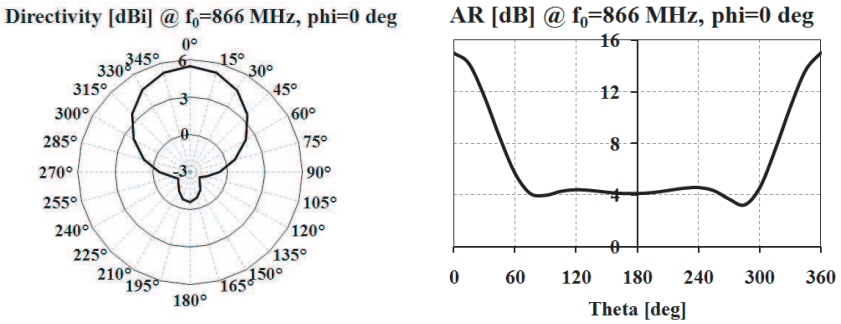

(a) (b)

Figure 5. Numerical results calculated for the radiation properties of the patch illustrated in Fig. 4(a).

the patch has an elliptical polarization with an Axial Ratio (AR) of about 4 dB (see Fig. 5).

2.2. Parasitic Patch Design

The approach used to reconfigure the radiation pattern of the active patch presented in the previous part of this section is the one suggested in [25], where a switchable Yagi-Uda antenna is proposed. More in details, in [25] the main beam direction of a planar three elements array is switched by using two parasitic dipoles with reconfigurable length.

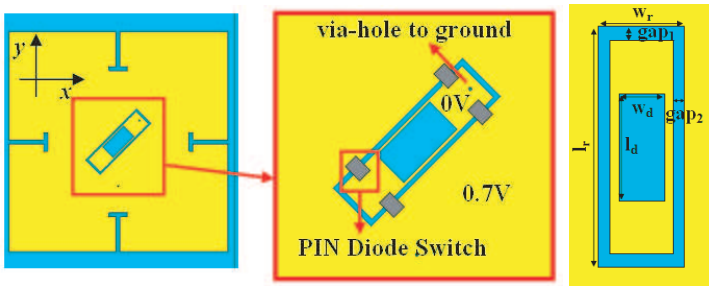

Figure 6. Geometry of the patch used as parasitic element of the proposed SPA.

This way, the antenna behaves as a Yagi-Uda antenna in which the dipole working as a director and the one working as a reflector can be exchanged. Similarly, the idea here suggested is to switch the main beam direction of the active patch by means of parasitic patches with a reconfigurable operating frequency so that they can work as reflector or director.

More specifically, the reconfigurability of the resonance frequency of the parasitic patches was obtained by means of four PIN diodes switches (the HMPP-389X diodes by Avago®) used to vary the length of the slot on the diagonal (see Fig. 6). The values of the geometric parameters (see Fig. 6) of the slot on the parasitic patch assumed as starting point of the SPA design were:

$$w_d = 0.61 w_{\text{slot}}, \quad l_d = 0.68 l_{\text{slot}}; \quad w_r = 1.21 w_{\text{slot}}, \quad l_r = 1.36 l_{\text{slot}}$$

where w_{slot} and l_{slot} are the dimensions of the slot of the active patch given in Table 1.

Referring to Fig. 6, the off-state of the switches corresponds to larger dimensions of the slot ($l_r \times w_r$) and then to a lower frequency of resonance, while the on-state corresponds to smaller dimensions of the slot ($l_d \times w_d$) and then to a higher frequency of resonance. In fact, the operating frequency of a slotted patch depends on the slot length and it lowers as the slot length increases.

This is highlighted in Fig. 7 where full-wave simulation results obtained for the geometry of the parasitic patch illustrated in Fig. 6 are shown. More specifically, the reflection coefficients calculated for the two useful configurations of the switches, corresponding to the reflector (all switches in the off-state) and to the director configuration (all switches in the on-state), are given and compared with the reflection coefficient of the active patch. As expected, it can be noticed that, when the parasitic patch is in the reflector configuration, the

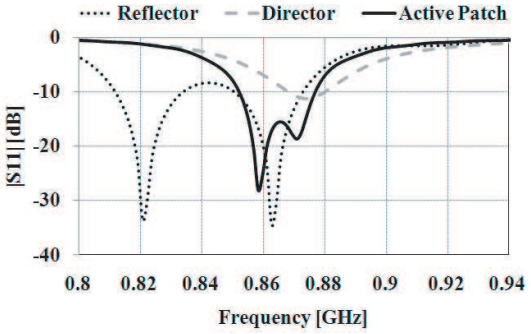

Figure 7. Comparison between the reflection coefficient corresponding to the active patch and the ones calculated for the parasitic patch in the reflector and director configuration. Referring to the geometry of the parasitic patch illustrated in Fig. 8, the director configuration is the one corresponding to the four diodes in the on-state; while the reflector configuration is the one corresponding to the four diodes in the off-state.

resonance frequencies of the two orthogonal modes associated to the slot move away from each other and shift toward lower frequencies. Conversely, when the patch is in the director configuration, the resonance frequencies of the two orthogonal modes become closer and shift toward higher frequencies.

It is worth underlining that, thanks to the use of slotted patches instead of dipoles, with respect to the approach presented in [25], the one suggested in this paper allows to obtain higher values of the gain and an elliptical polarization [10].

3. SWITCHED PARASITIC ARRAY: EXPERIMENTAL AND NUMERICAL RESULTS

As a proof of concept of the SPA design strategy proposed in this paper, a mono-dimensional array consisting of three elements was optimized and realized. Photographs of the realized prototype are given in Fig. 8. The use of three elements corresponds to three useful configurations:

1) the parasitic patch on the left and on the right configured so to work as a reflector and a director, respectively (RAD configuration);
2) the parasitic patch on the left and on the right configured so to work as a director and a reflector, respectively (DAR configuration);

(a) (b)

Figure 8. Proposed SPA: (a) photographs of the realized three-element prototype and (b) experimental setup used for scattering parameters measurements.

3) both the parasitic patches configured to work as a reflector (RAR configuration).

The RAR configuration was preferred to the DAD one (Director-Active Director) because from full-wave simulations it seemed more suitable to obtain a broadside radiation pattern.

The final geometry was the result of full-wave optimizations of the dimensions of the slot on the parasitic patches and of the distance between the array elements. The goals of optimizations were: a) to maximize and make symmetric the tilt with respect to the broadside direction of the main lobe direction corresponding to RAD and DAR configurations, b) to achieve in all configurations a good level of matching and an elliptical polarization at 866 MHz. The dimensions of the final geometry obtained this way are summarized in Table 1. Measurements of the reflection coefficient corresponding to the three possible configurations were performed by using the experimental setup illustrated in Fig. 8 and verified by means of a Time Domain Reflectometry approach [42–48]. Results obtained this way were in a perfect agreement; they are summarized in Fig. 9 and compared with numerical data. It can be seen that at 866 MHz values of the reflection coefficient lower than −1 dB were obtained in all configurations.

Experimental data obtained for radiation patterns in the H-plane are illustrated in Fig. 10; the directivity is of about 6 dBi in all configurations. In the H-plane, the main lobe direction is at $-30°$ in the DAR configuration, at $0°$ in the RAR configuration and at $+30°$ in the RAD configuration.

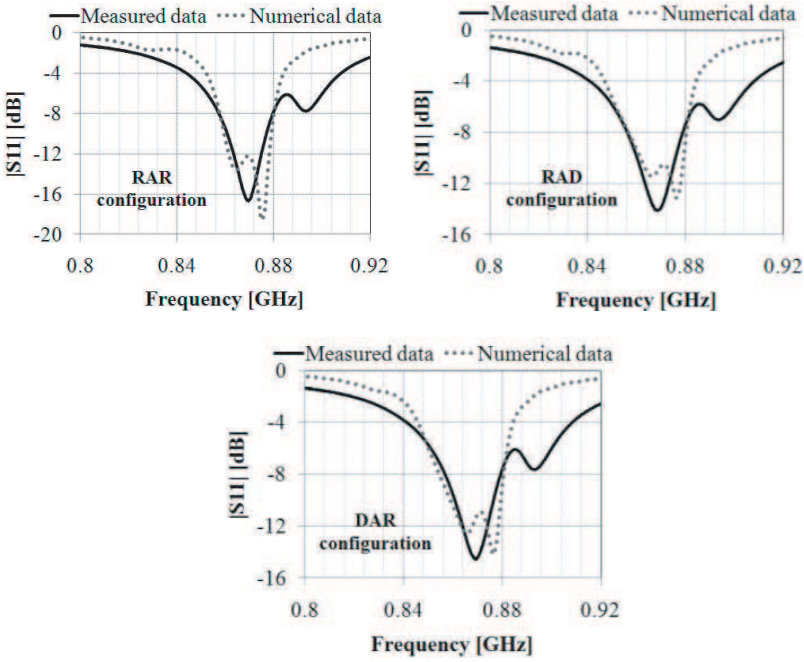

Figure 9. Experimental data of the reflection coefficient of the prototype shown in Fig. 8. Measurements were performed for each of the three possible configurations of the array by using the experimental setup illustrated in Fig. 8.

The dependence on the properties of the patch substrate (electric permittivity and thickness) of these results was also investigated by means of full-wave simulations. Fig. 11 summarizes results obtained for the case of a substrate consisting of: 1) a single layer of FR4 laminate with a thickness of 4 mm, 2) a single layer of poliver with a thickness of 4 mm. It has been verified that both the use of a thinner substrate and a substrate with higher values of the electric permittivity result in smaller values of the tilt with respect to the broadside direction of the main lobe corresponding to RAD and DAR configurations. In fact, from numerical data the tilt was $\pm 10^\circ$ and $\pm 40^\circ$ for an FR4 and a poliver substrate, respectively.

Finally, the possibility to extend to five the number of possible configurations by using a bi-dimensional array was studied. More specifically, we investigated the two SPAs illustrated in Fig. 12 corresponding to the alignment of the parasitic patch along the active patch diagonals (see Fig. 12(a)) and to the E-/H-plane of the active

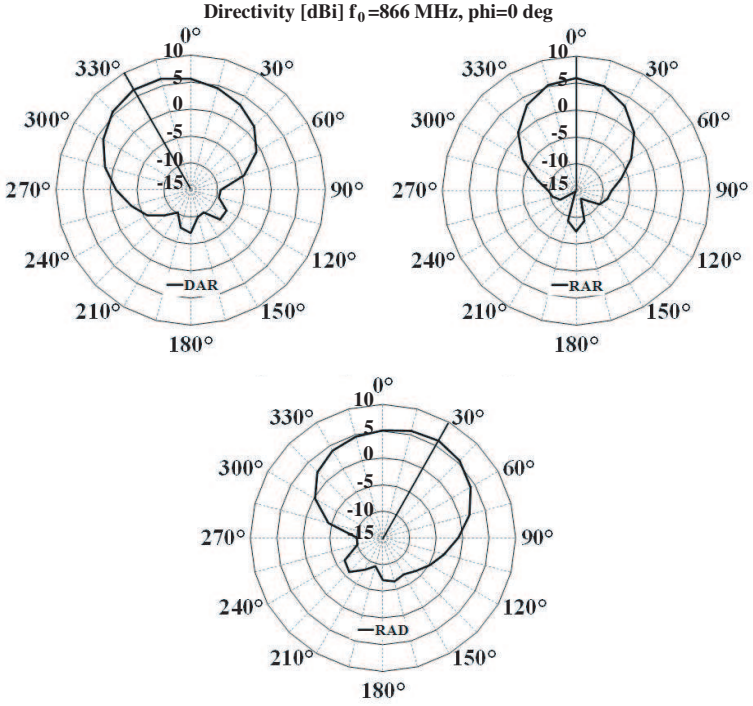

Figure 10. Experimental data of the radiation pattern obtained for the three possible configurations of the proposed SPA.

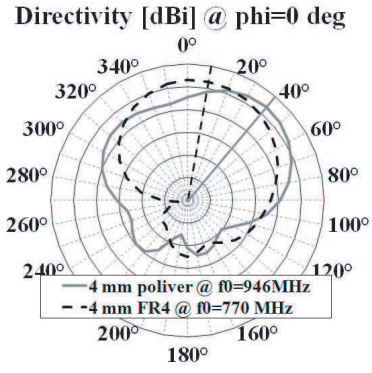

Figure 11. Numerical results corresponding to the use of different substrates: comparison between the radiation patterns in the RAD configuration calculated at the resonance frequency.

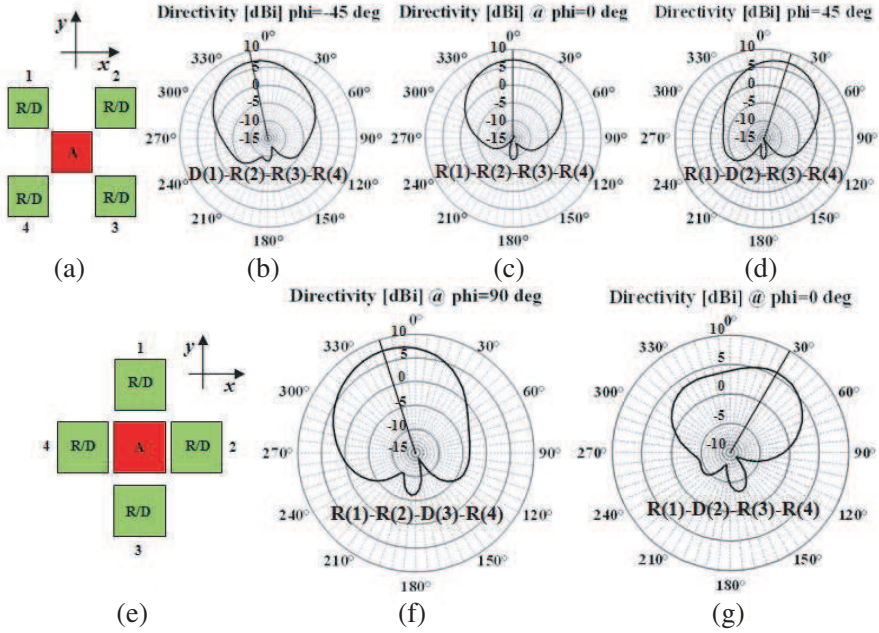

Figure 12. Application of the proposed approach for designing bi-dimensional arrays: investigated configurations and numerical results calculated for the radiation patterns.

patch (see Fig. 12(e)). In both cases, configurations used to obtain a tilt of the main lobe direction with respect to the broadside direction were obtained by setting three of the four parasitic patches as reflectors and only one as director. Corresponding results are given in Fig. 12; the SPA illustrated in Fig. 12(a) allows to obtain a tilt of $\pm 12°$, $0°$, $\pm 18°$ (see Figs. 12(b)–(d)), while the SPA illustrated in Fig. 12(e) allows to obtain a tilt of $\pm 18°$, $0°$, $\pm 30°$ (see Figs. 12(b)–(d)). It is worth underlining that these results were obtained by using for the parasitic patches the dimensions calculated for optimum operation of the mono-dimensional array. As a consequence, results given in Fig. 12 could be improved by optimizing the parasitic patches so to make symmetric the tilt which corresponds to the useful configurations of the SPA.

4. CONCLUSION

A switched parasitic array based on the use of a compact slotted microstrip patch has been proposed. Reconfigurability of the radiation pattern is obtained by varying the length of the slot on the parasitic

patches by means of four PIN diodes. Experimental data referring to a prototype consisting of an array of three elements have been presented and discussed. It is demonstrated that the proposed array has a main beam direction that can be switched in the H-plane through three different configurations. Numerical data demonstrating the suitability of the proposed approach to be applied to obtain a larger number of possible configurations have been also reported.

REFERENCES

1. Monti, G., L. Tarricone, and L. Corchia, "MEMS-based filter with a reconfigurable band-pass," *Proc. European Conference on Antennas and Propagation, EuCAP*, 445–448, 2009.
2. Monti, G., R. De Paolis, and L. Tarricone, "Design of a 3-state reconfigurable CRLH transmission line based on MEMS switches," *Progress In Electromagnetics Research*, Vol. 95, 283–297, 2009.
3. Marcaccioli, L., P. Farinelli, M. M. Tentzeris, J. Papapolymerou, and R. Sorrentino, "Design of a broadband MEMS-based reconfigurable coupler in Ku-band," *Proc. 38th Europ. Microw. Conf.*, 595–598, 2008.
4. Zheng, S., W. Chan, and Y. Wong, "Reconfigurable RF quadrature patch hybrid coupler," *IEEE Trans. on Industrial Electronics*, Vol. PP, No. 99, 2012.
5. Monti, G., R. De Paolis, and L. Tarricone, "Dual-band T-junction with a reconfigurable power ratio," *Proc. 39th Europ. Microw. Conf., EuMC*, 1219–1222, 2009.
6. Corchia, L., G. Monti, and L. Tarricone, "MEMS reconfigurable bandpass filter," *Microw. and Optical Technology Letters,* Vol. 50. No. 8, 2096–2099, Aug. 2008.
7. Singh, G. and M. Kumar, "Design of frequency reconfigurable microstrip patch antenna," *6th IEEE Intern. Conf. on Industr. and Inf. Syst.*, Kandy, Sri Lanka, Aug. 2011.
8. Tariq, A. and H. Ghafouri-Shiraz, "Frequency-reconfigurable monopole antennas," *IEEE Trans. on Ant. and Propag.*, Vol. 60, No. 1, 44–50, 2012.
9. Huff, G. H., J. Feng, S. Zhang, and J. T. Bernhard, "A novel radiation pattern and frequency reconfigurable single turn square spiral microstrip antenna," *IEEE Microw. and Wireless Compon. Lett.*, Vol. 13, No. 2, 57–59, Feb. 2003.
10. Monti, G., L. Corchia, and L. Tarricone, "Patch antenna with reconfigurable polarization," *Progress In Electromagnetics Research C*, Vol. 9, 13–23, 2009.

11. Chen, S.-H., J.-S. Row, and K.-L. Wong, "Reconfigurable square-ring patch antenna with pattern diversity," *IEEE Trans. on Ant. and Propag.*, Vol. 55, No. 2, 2007.
12. Wu, W., B.-Z. Wang, X.-S. Yang, and Y. Zhang, "A pattern-reconfigurable planar fractal antenna and its characteristic-mode analysis," *IEEE Ant. and Propag. Magaz.*, Vol. 49, No. 3, 2007.
13. Costantine, J., Y. Tawk, C. G. Christodoulou, and S. B. Barbint, "A star shaped reconfigurable patch antenna," *IEEE MTT-S Intern. Microw. Work Series on Signal Integrity and High-speed Interconn.*, 2009.
14. Monti, G., L. Corchia, and L. Tarricone, "Planar bowtie antenna with a reconfigurable radiation pattern," *Progress In Electromagnetics Research C*, Vol. 28, 61–70, 2012.
15. Chung, K., Y. Nam, T. Yun, and J. Choi, "Reconfigurable microstrip patch antenna with switchable polarization," *ETRI Journal*, Vol. 28, 379–382, Jun. 2006.
16. Piazza, D., P. Mookiah, M. D'Amico, and K. R. Dandekar, "Pattern and polarization reconfigurable circular patch antenna for MIMO systems," *3rd Europ. Conf. on Antenna and Propag, EUCAP*, 1047–1051, Berlin, Germany, 2009.
17. Coetzee J. C. and Y. Liu, "Compact multiport antenna with isolated ports," *Microw. and Optical Techn. Lett.*, Vol. 50, No. 1, 229–232, 2007.
18. Shoaib,I., X. Chen, and Z. Ying, "A pattern reconfigurable dielectric resonator antenna array for adaptive MIMO systems," *Loughb. Ant. & Propag. Conf., LAPC*, 1–4, 2011.
19. Yan, S. and T. Chu, "A beam-steering and switching antenna array using a coupled phaselocked loop array," *IEEE Trans. on Ant. and Propag.*, Vol. 57, No. 3, 638–644, 2009.
20. Chen, W. H., J. W. Sun, X. Wang, Z. H. Feng, F. L. Chen, Y. Furuya, and A. Kuramoto, "A novel planar switched parasitic array antenna with steered conical pattern," *IEEE Trans. on Ant. and Propag.*, Vol. 55, No. 6, Jun. 2007.
21. Sun, C. and N. C. Karmakar, "Direction of arrival estimation based on a single port smart antenna using MUSIC algorithm with periodic signals," *Intern. Journ. of Inform. and Commun. Engin.*, 153–162, 2005.
22. Wennstrom, M. and T. Svantesson, "An antenna solution for MIMO channels: The switched parasitic antenna," *12th IEEE Intern. Symp. on Personal, Indoor and Mobile Radio Communic.*, Vol. 1, 159–163, 2001.

23. Preston, S. L., D. V. Thiel, T. A. Smith, S. G. O'Keefe, and J. W. Lu, "Base-station tracking in mobile communications using a switched parasitic antenna array," *IEEE Trans. on Ant. and Propag.*, Vol. 46, No. 6, 841–844, Jun. 1998.
24. Zhang, S., G. H. Huff, G. Cung, and J. T. Bernhard, "Three variations of a pattern reconfigurable microstrip parasitic array," *Microw. and Optical Techn. Lett.*, Vol. 45, No. 5, 2005.
25. Zhang, S., G. H. Huff, J. Feng, and J. T. Bernhard, "A pattern reconfigurable microstrip parasitic array," *IEEE Trans. on Ant. and Propag.*, Vol. 52, No. 10, Oct. 2004.
26. Urata,Y., M. Haneishi, and Y. Kimura, "Beam-adjustable planar arrays composed of microstrip antennas," *Electron. Comm. Jpn.*, Vol. 87, No. 10, 1–12, 2004.
27. Monti, G., F. Congedo, D. De Donno, and L. Tarricone, "Monopole-based rectenna for microwave energy harvesting of UHF RFID systems," *Progress In Electromagnetics Research C*, Vol. 31, 109–121, 2012.
28. Karmakar, N. C., S. M. Roy, and M. S. Ikram, "Development of smart antenna for RFID reader," *IEEE Intern. Conf. on RFID*, Las Vegas, Apr. 2008.
29. Monti, G. and F. Congedo, "UHF rectenna using a bowtie antenna," *Progress In Electromagnetics Research C*, Vol. 26, 181–192, 2011.
30. Hong, W., N. Behdad, and K. Sarabandi, "Tri-band reconfigurable antenna for RFID applications," *Proc. IEEE Ant. and Propag. Society Intern. Symp.*, 2669, 2006.
31. Monti, G., L. Catarinucci, and L. Tarricone, "Compact microstrip antenna for RFID applications," *Progress In Electromagnetics Research Letters*, Vol. 8, 191–199, 2009.
32. Catarinucci, L., R. Colella, and L. Tarricone, "Design, development, and performance evaluation of a compact and long-range passive UHF RFID tag," *Microw. and Optical Techn. Lett.*, Vol. 54, No. 5, 1335–1339, 2012.
33. De Donno, D., F. Ricciato, L. Catarinucci, and L. Tarricone, "Design and applications of a software-defined listener for UHF RFID systems," *IEEE MTT-S International Microwave Symposium Digest*, Baltimore, MD, USA, Jun. 2011.
34. Ali, J. K., "A new compact size microstrip patch antenna with irregular slots for handheld GPS application," *Eng. & Technology*, Vol. 26, No. 10, 2008.
35. Nageswara Rao, P. and N. V. S. N. Sarma, "A single feed circularly

polarized fractal shaped microstrip antenna with fractal slot," *PIERS Proceedings*, 195–197, Hangzhou, China, Mar. 24–28, 2008.

36. Islam, M. T., N. Misra, M. N. Shakib, and M. N. A. Zamri, "Circularly polarized microstrip patch antenna," *Information Technology Journal*, Vol. 9, No. 2, 363–366, 2010.
37. Cheng, H.-Q., L.-B. Tian, and B.-J. Hu, "Compact circularly polarized square microstrip fractal antenna with symmetrical T-slits," *Proc. Intern. Conf. on Wireless Commun., Network. and Mobile Comp., WiCom 2007*, 613–616, China, 2007.
38. De Donno, D., A. Esposito, G. Monti, and L. Tarricone, "Iterative solution of linear systems in electromagnetics (and not only): Experiences with CUDA," *Lecture Notes in Computer Science (including subseries Lect. Notes in Artificial Intelligence and Lect. Notes in Bioinformatics) 6586 LNCS*, 329–337, 2011.
39. De Donno, D., A. Esposito, G. Monti, and L. Tarricone, "Efficient acceleration of sparse MPIE/MoM with graphics processing units," *European Microw. Week 2011: "Wave to the Future", Conf. Proc. — 41st European Microw. Conf., EuMC*, 175–178, 2011.
40. De Donno, D., A. Esposito, G. Monti, and L. Tarricone, "GPU-based acceleration of MPIE/MoM matrix calculation for the analysis of microstrip circuits," *Proc. of the 5th European Conf. on Antennas and Propag., EUCAP*, 3921–3924, 2011.
41. De Donno, D., A. Esposito, G. Monti, and L. Tarricone, "Parallel efficient method of moments exploiting graphics processing units," *Microw. and Optical Techn. Lett.*, Vol. 52, No. 11, 2568–2572, 2010.
42. Catarinucci, L., G. Monti, and L. Tarricone, "A parallel-grid-enabled variable-mesh FDTD approach for the analysis of slabs of double-negative metamaterials," *IEEE Antenn. and Propag. Society, AP-S Intern. Symp. (Digest)*, 782–785, 2005.
43. Cataldo, A., G. Monti, E. De Benedetto, G. Cannazza, L. Tarricone, and L. Catarinucci, "Assessment of a TD-based method for characterization of antennas," *IEEE Trans. on Instrumentation and Measurement*, Vol. 58, No. 5, 1412–1419, May 2009.
44. Cataldo, A., E. De Benedetto, G. Cannazza, and G. Monti, "A reliable low-cost method for accurate characterization of antennas in time domain," *Metrology and Measurement Systems*, Vol. 15, No. 4, 571–583, 2008.
45. Cataldo, A., G. Monti, E. De Benedetto, G. Cannazza, L. Tarricone, and L. Catarinucci, "A comparative analysis of

reflectometry methods for characterization of antennas," *Proc. IEEE Instrum. Meas. Technol. Conf.*, 240–243, 2008.

46. Cataldo, A., G. Monti, E. De Benedetto, G. Cannazza, and L. Tarricone, "A noninvasive resonance-based method for moisture content evaluation through microstrip antennas," *IEEE Trans. on Instrument. and Measurem*, Vol. 58, No. 5, 1420–1426, 2009.
47. Cataldo, A., G. Monti, G. Cannazza, E. De Benedetto, L. Tarricone, and M. Cipressa, "A non-invasive approach for moisture measurements through patch antennas," *Proc. of IEEE Instrumentation and Measurem. Technology Conf.*, 1012–1015, 2008.
48. Monti, G., L. Corchia, and L. Tarricone, "ISM band rectenna using a ring loaded monopole," *Progress In Electromagnetics Research C*, Vol. 33, 1–15, 2012.